

Spontaneous emergence of large-scale cell cycle synchronization in amoeba colonies

This content has been downloaded from IOPscience. Please scroll down to see the full text.

2014 Phys. Biol. 11 036001

(<http://iopscience.iop.org/1478-3975/11/3/036001>)

View [the table of contents for this issue](#), or go to the [journal homepage](#) for more

Download details:

IP Address: 132.236.27.111

This content was downloaded on 19/04/2014 at 11:33

Please note that [terms and conditions apply](#).

Spontaneous emergence of large-scale cell cycle synchronization in amoeba colonies

Igor Segota, Laurent Boulet, David Franck and Carl Franck

Laboratory of Atomic and Solid State Physics, Cornell University, Ithaca, NY 14853, USA

E-mail: is246@cornell.edu

Received 1 October 2013, revised 11 February 2014


Accepted for publication 10 March 2014

Published 15 April 2014

Abstract

Unicellular eukaryotic amoebae *Dictyostelium discoideum* are generally believed to grow in their vegetative state as single cells until starvation, when their collective aspect emerges and they differentiate to form a multicellular slime mold. While major efforts continue to be aimed at their starvation-induced social aspect, our understanding of population dynamics and cell cycle in the vegetative growth phase has remained incomplete. Here we show that cell populations grown on a substrate spontaneously synchronize their cell cycles within several hours. These collective population-wide cell cycle oscillations span millimeter length scales and can be completely suppressed by washing away putative cell-secreted signals, implying signaling by means of a diffusible growth factor or mitogen. These observations give strong evidence for collective proliferation behavior in the vegetative state.

Keywords: cell cycle, *Dictyostelium discoideum*, collective behavior, synchronization

 Online supplementary data available from stacks.iop.org/PhysBio/11/036001/mmedia

Introduction

Collective oscillations of entire populations characterize many biological processes such as synchronized flashing of fireflies [1], glycolytic oscillations in yeast [2], cell aggregation in amoebae [3], circadian rhythms in cyanobacteria [4, 5], somite segmentation in zebrafish embryos [6], nuclear division in multinuclear HeLa cells [7] and synchronized cleavage divisions in *Xenopus* frog embryos [8]. These cooperative interactions can provide a fitness advantage, e.g. in cases when the environment is depleted of nutrients [3] or to assist in mate finding [1]. Recently, there has been substantial progress in synthetic biology with the goal of engineering oscillatory genetic networks [9] and coupling them by quorum sensing [10]. In this work, however, the focus is on naturally emergent collective behavior in a model unicellular eukaryote, *Dictyostelium discoideum*. In nature, *D. discoideum* lives in the soil and feeds on bacteria in their vegetative growth state [11]. Keating and Bonner [12] and Kakebeeke *et al* [13] showed that vegetative cells can interact by repelling each other and Phillips and Gomer [14] later identified AprA as an autocrine chemorepellant in vegetative cells. When starved of nutrients *D. discoideum* transitions to a collective state

by chemotactically grouping into multicellular aggregates of 10^5 cells, eventually differentiating into stalk and spore cells, forming a lifeboat for their genomes. However, in comparison to yeast *S. cerevisiae* [15] or *Xenopus* [16], researchers still do not have a full array of cell cycle markers for *D. discoideum* [17, 18]. The first live-cell S-phase marker has only recently been introduced in *D. discoideum* [19].

Results

We studied *D. discoideum* population dynamics on glass substrates. A typical example of the dynamics of the average cell surface density in the exponentially growing regime of the vegetative phase was obtained by automated counting (figure 1(a)). Potentially interesting features are any deviations from pure exponential growth that do not result from uncertainty in counting. Here, the initial cell count is 40 ± 2 cells, spread out uniformly over a 4 mm^2 viewing area. During 26 h, the cells did not move significantly ($200 \mu\text{m}$) compared to our $2.3 \text{ mm} \times 1.8 \text{ mm}$ recording area, resulting in patchy growth (figure 1(b)) further investigated in [20].

First, we show that the deviations from exponential growth (figure 1(a)) indeed represent signatures of collective

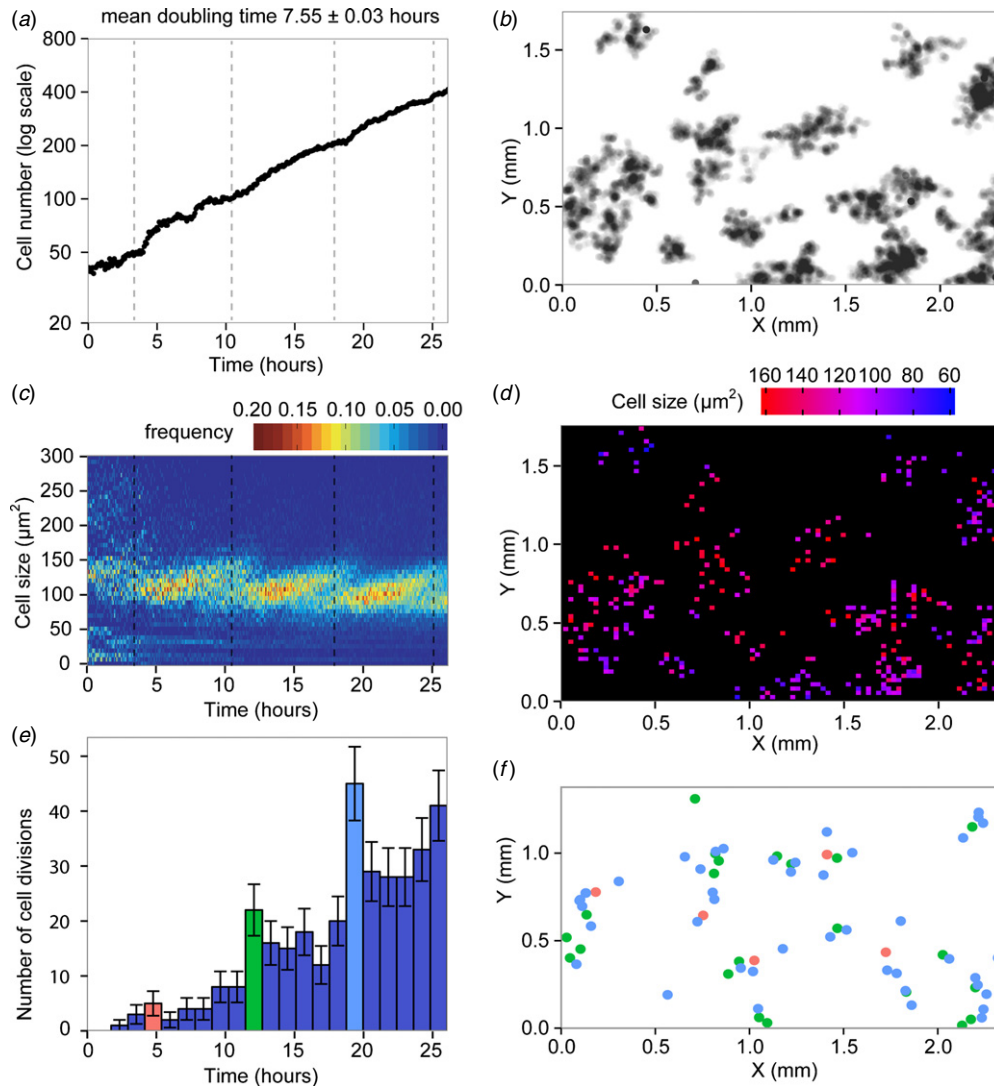


Figure 1. Synchronization of cell growth on a substrate. (a) Overall population of proliferating cells versus time showing apparently featureless dynamics, (b) strobe (at 5 min intervals over 26 h) image of cell positions; darker areas correspond to more visited locations. (c) Dynamics of cell size distribution showing clear evidence for cell cycle synchronization after about 4 h. The sudden jumps are marked by dashed lines, at times also indicated in (a). (d) Spatial distribution of cells at 25 h with color representing cell size. (e) Number of cell divisions in 1.2 h intervals. Peaks in cell divisions correlate with sudden jumps in the cell size distribution shown in (c). Error bars show the upper limit for the counting uncertainty calculated from Poisson noise. (f) Spatial distribution of the three cell division peaks from (e), with matching colors.

cell divisions, by measuring the time dynamics of cell size distribution (figure 1(c)). This approach was recently used to quantify induced cell synchronization [21]. The time dynamics of cell size distributions (figure 1(c)) shows a clear periodic pattern, demonstrating partial synchrony in cell growth. To ensure that this is not a lineage effect (i.e. arising from a low number subpopulation), we show the entire viewing area binned into $27 \mu\text{m}$ wide squares, with each bin color-coded by the local cell size and averaged over 1–2 cells (figure 1(d)). This demonstrates that synchronization in cell growth is not localized to a particular patch, thereby excluding any possibility of a lineage effect alone causing the large-scale oscillations. The cell-to-cell variation in doubling times is 7.3 ± 0.8 h (figure S4, available from stacks.iop.org/PhysBio/11/036001/mmedia), which is reflected in a strong lineage effect in a

monoclonal population (see supplementary data, available from stacks.iop.org/PhysBio/11/036001/mmedia).

Next, we ensured that this periodic growth correlates with cell divisions. We manually annotated all cell division events, omitting initial events corresponding to declustering of cell clusters and cytokinesis of multinuclear cells present in suspension cultures [22], only counting single cell splitting into two, preceded by rounding up at the onset of cytokinesis. These manual annotations agree within $<1\%$ with automated counts: for the data presented in figure 1, we counted 343 cell division events compared to 344 particles detected by automated counting (excluding initial declustering events). The same was repeated for two other experiments (see section 3 in the supplementary data, available from stacks.iop.org/PhysBio/11/036001/mmedia). The cell division dynamics shows clear pulses (figure 1(e)) correlated with the

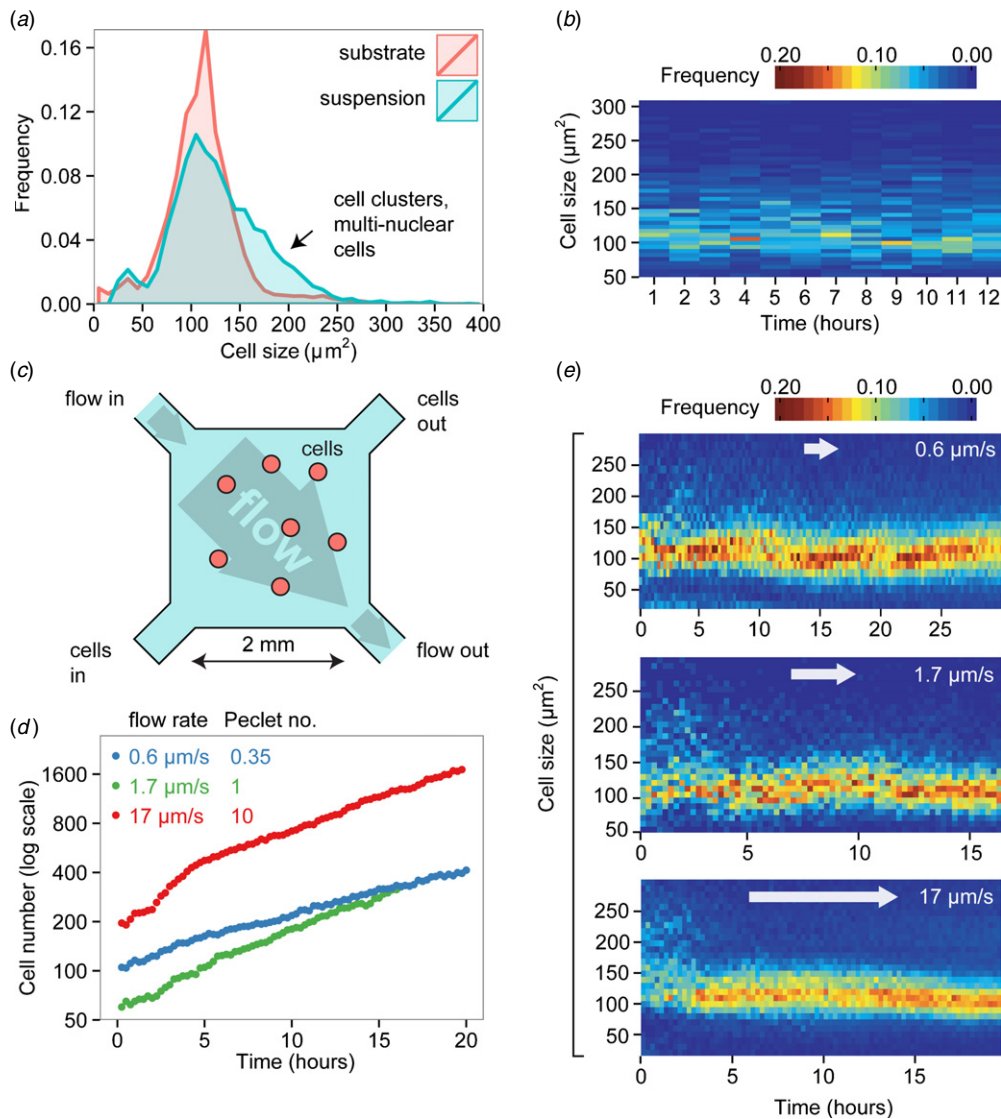


Figure 2. Suspension culture growth and microfluidic flow experiments. (a) Time averaged cell size distributions for substrate and suspension growth. (b) Time course of cell size distribution in suspension. (c) Schematic of the microfluidic device employed for flow experiments. (d) Growth dynamics in flow experiments. (e) Time course of cell size distributions for substrate flow experiments.

beginnings of cell growth pulses (figure 1(c)). Furthermore, each collective cell division pulse (colored dots, figure 1(e)) is not localized to a particular patch (figure 1(f)). However, this still does not exclude the possibility of spontaneous synchronization in suspension cultures, which were used to grow cells before plating.

The cells grown in suspensions have a broader size distribution (figure 2(a)) than those on substrates, consistent with previous observations of cell clusters [23] and multinuclear cells [22]. These are all counted as a single particle by automated counting (figure 1(a)), however they are easily discriminated by cell size (particles between 150 and 300 μm^2 in figure 1(c)). Measurements of the cell size distribution dynamics in suspension cultures show no synchronized growth (figure 2(b)), consistent with previous observations in development of *D. discoideum* synchronization protocols [24, 18] showing no evidence for suspension cell synchronization. Our repeat experiments (see figure S1,

available from stacks.iop.org/PhysBio/11/036001/mmedia) clearly confirm the onset of synchronization on substrates.

Nevertheless, one might wonder whether this synchronization is an artifact of simultaneous cytokinesis of multinuclear cells and cell cluster disintegration, resulting in a sudden large increase in the number of single cells. Rather, we observed that multinuclear cells undergo cytokinesis and clusters disintegrate uniformly in time throughout the first 6 h after plating (see supplementary video, available from stacks.iop.org/PhysBio/11/036001/mmedia). This is also reflected in the fact that we do not observe a sudden large increase in the single cell number after the initial incoherent period (figures 1 and S1 (available from stacks.iop.org/PhysBio/11/036001/mmedia)), demonstrating that cell synchronization is not induced by plating. Previous studies in *D. discoideum* have shown that cytokinesis C, which is responsible for cell division of multinuclear cells, is cell cycle-uncoupled and adhesion-dependent [25–27], in agreement with our observations.

Next, we investigate the possibility that cells secrete a growth factor or a mitogen that serves as a synchronization signal. We first analyzed the microfluidic experiments we performed previously [23] with cells grown on a substrate in a PDMS microfluidic device (figure 2(c)). In these experiments the cells naturally adhered to the glass while fresh growth medium flowed above them with 0.6, 1.7 and 17 $\mu\text{m s}^{-1}$ flow speeds. The shear stresses the cells were exposed to in these flowing experiments were at least two orders of magnitude smaller than the shear stresses needed to induce mechanical responses in *D. discoideum* [28, 29] (for calculation see supplementary data section 7, available from stacks.iop.org/PhysBio/11/036001/mmedia) so it seems unlikely that the loss of coherence is due to the mechanical stress. As discussed later, in subsequent work, on a rare occasion we noticed a few cells advected by flow, presumably as daughters released by mitosis from the substrate. However, this occurred so rarely that it had no effect on our experiments where we had from about 50 to a few hundreds of cells. If the synchronization signal is a small signaling molecule with a diffusion coefficient of about 300 $\mu\text{m}^2 \text{s}^{-1}$, then these flow speeds correspond to Peclet numbers (see section 5, supplementary data (available from stacks.iop.org/PhysBio/11/036001/mmedia)), quantifying the ratio of advective to diffusive transport, on the order of 0.35 (diffusion dominated), 1 and 10 (advection dominated), respectively [23]. Again, we measured both the cell density dynamics (figure 2(d)) and the cell size distribution dynamics (figure 2(e)). This qualitatively demonstrates the loss of coherence with increasing flow speed. However, it does not quantify the degree of collective coherence or measure the population fraction locked into this collective rhythm.

In order to quantify the collective synchronization of N cells, we represented the cell cycle position of cell j as a unit vector in complex plane at angle θ_j (figure 3(a)). The collective cell cycle oscillations are then represented as N points running around a unit circle. The ‘order parameter’ $z = r e^{i\psi} = \frac{1}{N} \sum_{j=1}^N e^{i\theta_j}$ is a vector of the centroid of these N points whose radius r represents the degree of collective phase coherence and measures the oscillation magnitude of the entire population. If all the cells oscillate in unison, then the points are clustered together resulting in $r = 1$. For random phased cell oscillations, r is smaller but unlikely to approach zero unless N is very large. To address this, we calculated the average and the standard deviation of r for N randomly phased oscillators (supplementary data, available from stacks.iop.org/PhysBio/11/036001/mmedia).

Since cell growth and division are correlated in *D. discoideum* (comparing figures 1(d) and (e)), we defined the cell cycle phase θ_j to be proportional to the cell size a_j , i.e. $\theta_j = \frac{2\pi}{a_{\max} - a_{\min}} (a_j - a_{\min})$, with the minimum and maximum cell size approximated from the cell size distributions to be given by $a_{\min} = 80 \mu\text{m}^2$ and $a_{\max} = 150 \mu\text{m}^2$ (the results are robust with respect to changing limits a_{\min} and a_{\max}). Hence, the area ratio is $\frac{a_{\max}}{a_{\min}} = \frac{150}{80} \approx 1.88$, which is about a factor of two as expected, since the cells tend to flatten on a glass substrate. If the cells were shaped on a substrate as hemispherical caps then doubling their volume would cause

the area to increase by a factor of 1.6. The more flattened out the cells are the more the volume ratio would approach the surface area ratio, so our result does indicate some degree of flattening, consistent with our microscopic observations. The phase coherence r for the experiment analyzed in figure 1 shows periodic oscillations (figure 3(b)), which reflects the fact that the cell size distribution broadens between each collective cell division pulse. The peak-to-peak variation in r is about 0.15, with the observed maxima well above the expected value for an incoherent system of the same number of cells and minimum values corresponding to complete incoherency. However, in other experiments there remained some residual level of coherence at the minima (figures S1b and S1d, available from stacks.iop.org/PhysBio/11/036001/mmedia). The oscillations in r are possibly a consequence of the fact that while cell growth and division are coordinated, they are still separate processes and the synchronization signal might be a mitogen pulse that initiates cell division but does not persist throughout the majority of the cell cycle. While the true cell cycle phase is more precisely defined through the appearance of particular sets of cyclin proteins [30], no corresponding live-cell markers are available in *D. discoideum*. However it is still very unlikely that using the ‘true’ relation for $\theta_j(a_j)$ would erase all trace of the coherence observed here (figures 3(b), (c) and S1 (available from stacks.iop.org/PhysBio/11/036001/mmedia)).

We also calculated the phase coherence for the microfluidic flow experiments described above with AX3 cells and additional ones with AX4 cells in a 50% shorter chamber (see materials and methods section for details) and again confirm the loss of coherence with increasing flow speed—the phase coherence approaches the values expected for randomly phased oscillators (figure 3(c)). On rare occasions in the high flow regime we noticed cells advected by the flow. Since we observed no dependence of overall proliferation rate on flow rate here or in [23], we do not regard these events as having significance for the phase coherence values presented here. We compared the average phase coherence among experiments performed at different flow rates, and note that on average, phase coherence is higher at lower Peclet numbers (lower flow rates). The experiments were pooled into two groups based on the estimated Peclet numbers: low flow ($\text{Pe} \leq 0.35$) and high flow ($\text{Pe} \geq 1$). For each individual experiment we calculated the average phase coherence r and the average difference between the phase coherence r and its random-system average $r_{\text{incoherent}}$ (averaged over 15–20 h). As indicated in figures 3(d) and (e) we performed three low flow experiments and four high flow experiments with three and four data points, respectively. We first compared the average r values between these two groups using a two-tailed Welch two sample t -test, and obtained the p -value of 0.02. The same was also done for the difference between instantaneous r and its random-system average $r_{\text{incoherent}}$, and here we obtained the p -value of 0.01. Comparison between average values of r and $r_{\text{incoherent}}$, and its standard errors of the means for each of the performed experiments at different flow rates is shown in figures 3(d) and (e).

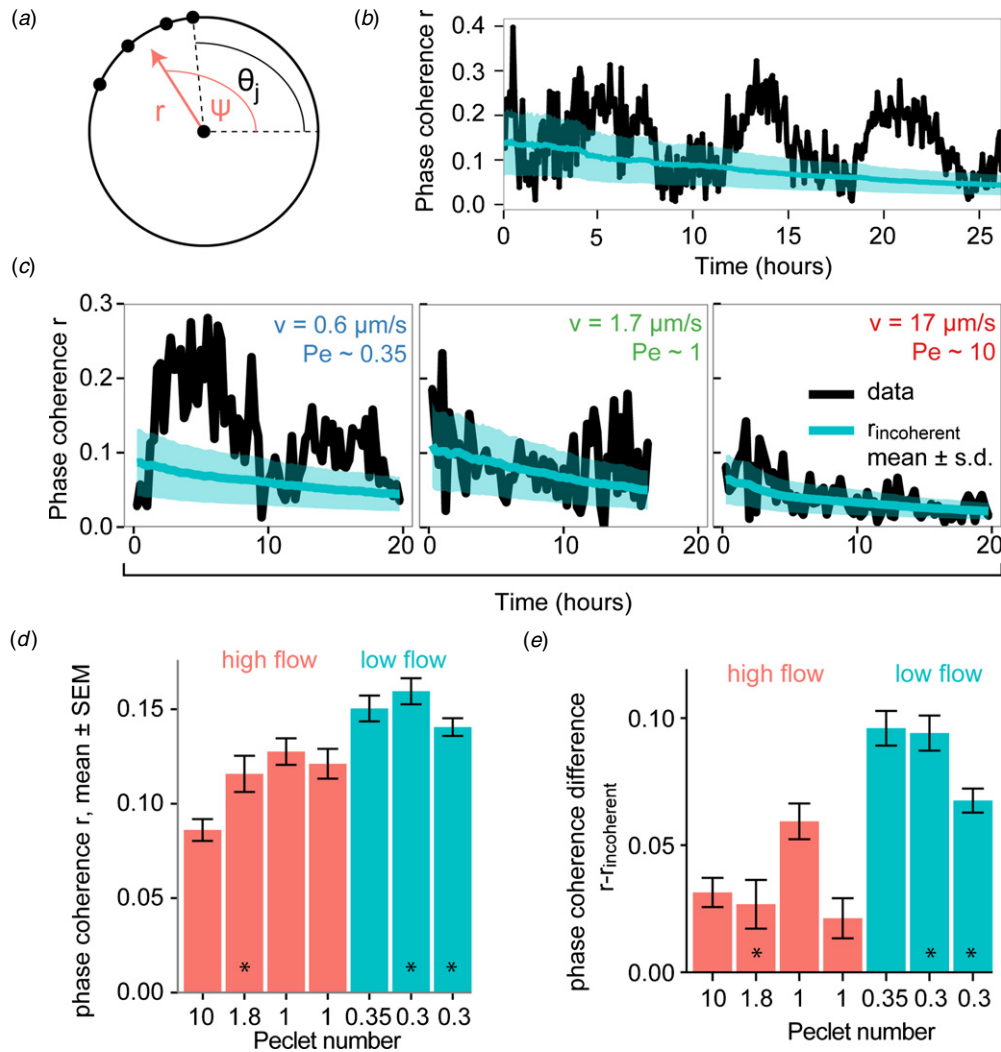


Figure 3. Quantitative analysis of oscillations. (a) Phase coherence r , a number between 0 and 1, is defined as the magnitude of the vector sum of N unit vectors each having an angle θ_j , divided by N (shown in red). The angle ψ describes the phase of the collective oscillation. (b) Phase coherence for the experiment in figure 1. The cells periodically go in and out of coherence. (c) Phase coherence for microfluidic flow experiments, demonstrating the loss of coherence at higher flow speeds. The cyan line and its spread denote the average and standard deviation for random-phase systems (see section 1, supplementary data (available from stacks.iop.org/PhysBio/11/036001/mmedia)). (d), (e) Phase coherence and its difference from the average for random-phase system as a function of Pelet number (flow rate). Error bars in both (d) and (e) show mean and its standard error. As noted, experiments in (d) and (e) were performed either with AX3 cells and 200 μm high microfluidic chamber (unmarked) or AX4 cells and 100 μm high microfluidic chamber (marked with asterisk). The flow rates were adjusted to ensure equal calculated Pelet numbers (section 5, supplementary data (available from stacks.iop.org/PhysBio/11/036001/mmedia)).

Discussion

Collective synchronization has been theoretically studied in various versions of the simple Kuramoto model [31–33]. The solution for the Kuramoto model for finite oscillator number predicts sustained coherence with increasing cell number, consistent with our shorter 25 h data (figure 3(b)), but inconsistent with our longer 40 h experiments (figure S1, available from stacks.iop.org/PhysBio/11/036001/mmedia). In addition, the observed feature of oscillating phase coherence (even if only in cell size) is not predicted by any of the Kuramoto models. These models assume that the coupling strength scales inversely with the number of oscillators, an assumption that needs to be changed in order to make realistic predictions for this system. Here, at least for short times, we expect that the coupling strength is diffusion limited and

independent of cell number. A more appropriate description of the synchronized dynamics presented here would also predict a spatial dependence of phase coherence. The onset of synchronization observed here (figures 1(c), 3(b) and S1 (available from stacks.iop.org/PhysBio/11/036001/mmedia)) occurs within a few hours, which is consistent with the approximately 4 h time needed for a small molecule with a diffusion coefficient of 300 $\mu\text{m}^2 \text{s}^{-1}$ to diffuse a distance of 2 mm and thereby cover the entire viewing field.

There is evidence for quorum sensing factors [34], growth factors and factors repressing cell proliferation in *D. discoideum* [35–37] and their potential role in synchronization remains to be determined. Furthermore, we speculate as to the possible purpose of these oscillations. It is known that during starvation, *D. discoideum* cells differentiate into prestalk and prespore cells, a process which correlates with

cell cycle positions [38–40]. Since only spore cells potentially survive, there is competition to form spores. If the cell fate is determined by its cell cycle position (they are certainly correlated), the synchronized fraction could be collectively turned into either prestalk or prespore cells and possibly more effectively competes for becoming spores.

The absence of spontaneously synchronized growth in suspensions might be caused by the fact that the lack of substrate may introduce a stochastic delay of cytokinesis by a time that is difficult to estimate. In addition, the suspension system is further complicated by the fact that cells can cluster [41], grow in 3D and that the presence of shear flow in orbital shakers can affect cytokinesis of multinuclear cells. The cytokinesis pathways are different in suspension and on a substrate (for an overview see [25]). In addition to the lack of oscillations, another difference in culturing cell populations between substrate and suspension growth was the lack of a lag phase on substrates, also previously observed [23]. As reported here, we have not observed any evidence of lagging even when the cells are plated at a very low surface density of around 0.25 cells/mm² (see section 6 in the supplementary data, available from stacks.iop.org/PhysBio/11/036001/mmedia).

As we indicated, these observations are ripe for quantitative modeling and present elegant challenges: macro-scale synchronization of proliferating oscillators where the micro-scale oscillator is the proliferation process itself. Future experimental work will reveal the extent to which this phenomenon is universal. From a practical standpoint, it presents insight into the problem of cell culturing for stem cell development and large-scale parallel bioassays where the difficulty of very dilute cell culture arises, as discussed in [23]. It also demands better appreciation of the importance of the nonliving culture environment: flowing suspension versus hydrophilic substrates with or without fluid flow. Equally interesting are the biochemical circuits in play, e.g. the timing pattern of the chemical signals that cells are apparently exchanging and the biological underpinnings of this process, i.e. how does this synchronization signal affect different phases of the cell cycle and what is the chemical identity of the putative signal molecule responsible for synchronization (based on the Peclet estimates presented here it may well be a small molecule)¹. Returning to the theoretical challenges, while we have argued that our observations reveal collective proliferation waves that already encompassed the entire field of view (figures 1(b) and (d)), our understanding of the spatial dynamics of these waves remains an open question.

Materials and Methods

D. discoideum wild-type AX3 and AX4 axenic strains were grown in HL5 with glucose suspension culture (ForMedium, UK) with 250 μ l PenStrep (Invitrogen) per 25 ml flask. No variation in results was noticed with cell subculturing for up to one year. Cells were grown in exponential phase on an orbital shaker (150 rpm) in standard 25 ml Erlenmeyer flasks to 10⁵ or 10⁶ cells/ml (21 °C). For substrate growth,

these cultures were transferred to fresh HL5, diluted to 10³–10⁵ cells/ml and 300 μ l samples were plated on hydrophilic MatTek (P50G-1.5-14-F) glass bottom dishes. Recording was performed in bright field with an inverted Olympus IX71 or an upright Nikon Optiphot (4 \times objective both) within 15 min of plating. Images were taken every 5 min using a Home Science Tools camera MI-DC5000 or a Logitech QuickCam Pro 4000. The Olympus/Home Science combination provided better resolution (figures 1 and S1a (available from stacks.iop.org/PhysBio/11/036001/mmedia)) than the Optiphot/Logitech system (figure S1c, available from stacks.iop.org/PhysBio/11/036001/mmedia). For suspension growth, flasks were sampled hourly for 11–12 h, by injecting a 20 μ l sample into a hemocytometer and \sim 20 image sets were taken within 3 min.

Background was removed using ImageJ (NIH) by subtracting the average of all images from each frame (for each experiment). Particles were detected and counted using ImageJ by thresholding. Cell sizes were measured using the ‘Analyze particles’ tool. Centroids of particles were used as cell coordinates (figures 1(c), (d) and (f)). The uncertainty in area measurements is roughly equal to our bin size, i.e. \pm 10 μ m in figure 1(c). Microfluidic experiments including imaging systems used were described previously [23]. Briefly, polydimethylsiloxane (PDMS) on glass substrate microfluidic devices (see figure 2(c), showing a typical configuration for loading exponential phase cells) were employed. The chamber dimensions were 2 mm \times 2 mm \times 200 μ m for AX3 cells and 2 mm \times 2 mm \times 100 μ m for AX4 cells (these are indicated in figures 3(d) and (e) as unmarked and asterisk-marked, respectively). After loading, fresh HL5 growth medium was flowed continuously in the direction indicated in the figure. There was no observable difference in behavior between AX3 and AX4 cells. Frames were recorded every 2.5–15 min for 16–40 h. Images were analyzed as described previously. The doubling times were 8–11 h, consistent with the usual suspension culturing. In an effort to suppress bubble formation in the microchamber, on occasion both HL5 supply and cell suspensions were degassed through rounds of volume increases in closed syringes and mechanical tapping.

Acknowledgments

We thank Dicty Stock Center; Northwestern University for AX3 and AX4 cell lines and Cornell Center for Materials Research for use of the facilities funded by the National Science Foundation under grant DMR-1120296.

IS designed the study. IS, LB, DF and CF performed the experiments. IS and CF analyzed the data and wrote the manuscript.

References

- [1] Buck J and Buck E 1968 Mechanism of rhythmic synchronous flashing of fireflies *Science* **159** 1319–27
- [2] De Monte S, d’Ovidio F and Sorensen P G 2007 Dynamical quorum sensing: population density encoded in cellular dynamics *PNAS* **104** 18377–81

¹ We thank the anonymous referee for this comment.

- [3] Sawai S, Thomason P A and Cox E C 2005 An autoregulatory circuit for long-range self-organization in *Dictyostelium* cell populations *Nature* **433** 323–6
- [4] Mihalcescu I, Hsing W and Leibler S 2004 Resilient circadian oscillator revealed in individual cyanobacteria *Nature* **430** 81–5
- [5] Yang Q, Pando B F, Dong G, Golden S S and van Oudenaarden A 2010 Circadian gating of the cell cycle revealed in single cyanobacterial cells *Science* **327** 1522–6
- [6] Horikawa K, Ishimatsu K, Yoshimoto E, Kondo S and Takeda H 2006 Noise-resistant and synchronized oscillation of the segmentation clock *Nature* **441** 719–23
- [7] Rao P N and Johnson R T 1970 Mammalian cell fusion: studies on the regulation of DNA synthesis and mitosis *Nature* **225** 159–64
- [8] Kirschner M, Newport J and Gerhart J 1985 The timing of early developmental events in *Xenopus* *Trends Genet.* **1** 41–47
- [9] Elowitz M B and Leibler S 2000 A synthetic oscillatory network of transcriptional regulators *Nature* **403** 335–8
- [10] Danino T, Mondragon-Palmino O, Tsimring L and Hasty J 2010 A synchronized quorum of genetic clocks *Nature* **463** 326–30
- [11] Kessin R H 2001 *Dictyostelium: Evolution, Cell Biology and the Development of Multicellularity* (Cambridge: Cambridge University Press)
- [12] Keating M T and Bonner J T 1977 Negative chemotaxis in cellular slime molds *J. Bacteriol.* **130** 144–7
- [13] Kakebeeke P I J, De Wit R J W, Kohtz D S and Konijn M T 1979 Negative chemotaxis in *Dictyostelium* and *Polysphondylium* *Exp. Cell Res.* **124** 429–33
- [14] Phillips J E and Gomer R H 2012 A secreted protein is an endogenous chemorepellant in *Dictyostelium discoideum* *Proc. Natl Acad. Sci. USA* **109** 10990–5
- [15] Cai L and Tu B P 2012 Driving the cell cycle through metabolism *Annu. Rev. Cell Dev. Biol.* **28** 59–87
- [16] Philpott A and Yew R P 2008 The *Xenopus* cell cycle: an overview *Mol. Biotechnol.* **39** 9–19
- [17] Weeks G and Weijer C J 1994 The *Dictyostelium* cell cycle and its relationship to differentiation *FEMS Microbiol. Lett.* **124** 123–30
- [18] Weijer C J, Duschl G and David C N 1984 A revision of the *Dictyostelium discoideum* cell cycle *J. Cell Sci.* **70** 111–31
- [19] Muramoto T and Chubb J R 2008 Live imaging of the *Dictyostelium* cell cycle reveals widespread S phase during development, a G2 bias in spore differentiation and a premitotic checkpoint *Development* **135** 1647–57
- [20] Houchmandzadeh B 2008 Neutral clustering in a simple experimental ecological community *Phys. Rev. Lett.* **101** 078103
- [21] Tzur A, Kafri R, LeBleu V S, Lahav G and Kirschner M W 2009 Cell growth and size homeostasis in proliferating animal cells *Science* **325** 167–71
- [22] Waddell D R, Duffy K and Vogel G 1987 Cytokinesis is defective in *Dictyostelium* mutants with altered phagocytic recognition, adhesion, and vegetative cell cohesion properties *J. Cell Biol.* **105** 2293–300
- [23] Franck C, Ip W, Bae A, Franck N, Bogart E and Le T T 2008 Contact-mediated cell-assisted cell proliferation in a model eukaryotic single-cell organism: an explanation for the lag phase in shaken cell culture *Phys. Rev. E* **77** 041905
- [24] Maeda Y 1986 A new method for inducing synchronous growth of *Dictyostelium discoideum* cells using temperature shifts *Microbiology* **132** 1189–96
- [25] Uyeda T Q P and Nagasaki A 2004 Variations on a theme: the many modes of cytokinesis *Curr. Opin. Cell Biol.* **16** 55–60
- [26] Hibi M, Nagasaki A, Takahashi M, Yamagishi A and Uyeda T Q 2003 *Dictyostelium discoideum* talin is a crucial for myosin OO-independent and adhesion-dependent cytokinesis *J. Muscle Res. Cell Motil.* **25** 127–40
- [27] Nagasaki A, de Hostos E L and Uyeda T Q 2002 Genetic and morphological evidence for two parallel pathways of cell-cycle-coupled cytokinesis in *Dictyostelium* *J. Cell Sci.* **115** 2241–51
- [28] Fache S, Dalous J, Engelund M, Hansen C, Chamaraux F, Fourcade B, Satre M, Devreotes P and Bruckert F 2005 Calcium mobilization stimulates *Dictyostelium discoideum* shear-flow-induced cell motility *J. Cell Sci.* **118** 3445–58
- [29] Decave E, Rieu D, Dalous J, Fache S, Brechet Y, Fourcade B, Satre M and Bruckert F 2003 Shear-flow induced motility of *Dictyostelium discoideum* cells on solid substrate *J. Cell Sci.* **116** 4331–43
- [30] Murray A W 2004 Recycling the cell cycle: cyclins revisited *Cell* **116** 221–34
- [31] Kuramoto Y and Nishikawa I 1987 Statistical macrodynamics of large dynamical systems. Case of a phase transition in oscillator communities *J. Stat. Phys.* **49** 569–605
- [32] Acebron J A, Bonilla L L, Perez Vicente C J, Ritort F and Spigler R 2005 The Kuramoto model: a simple paradigm for synchronization phenomena *Rev. Mod. Phys.* **77** 137–85
- [33] Strogatz S H 2000 From Kuramoto to Crawford: exploring the onset of synchronization in populations of coupled oscillators *Physica D* **143** 1–20
- [34] Gole L, Riviere C, Hayakawa Y and Rieu J-P 2011 A quorum-sensing factor in vegetative *Dictyostelium discoideum* cells revealed by quantitative migration analysis *PLoS ONE* **6** e26901
- [35] Gomer R H, Jang W and Brazill D 2011 Cell density sensing and size determination *Dev. Growth Differ.* **53** 482–94
- [36] Brock D A and Gomer R H 2005 A secreted factor represses cell proliferation in *Dictyostelium* *Development* **132** 4553–62
- [37] Whitbread J A, Sims M and Katz E R 1991 Evidence for the presence of a growth factor in *Dictyostelium discoideum* *Dev. Genet.* **12** 78–81
- [38] Gomer R H and Firtel R A 1987 Cell-autonomous determination of cell-type choice in *Dictyostelium* development by cell-cycle phase *Science* **237** 758–62
- [39] Araki T, Nakao H, Takeuchi I and Maeda Y 1994 Cell-cycle-dependent sorting in the development of *Dictyostelium* cells *Dev. Biol.* **162** 221–8
- [40] Wood S A, Ammann R R, Brock D A, Li L, Spann T and Gomer R H 1996 RtoA links initial cell type choice to the cell cycle in *Dictyostelium* *Development* **122** 3677–85
- [41] Loomis W F 1982 *The Development of Dictyostelium Discoideum* (New York: Academic) p 199